International Scholarly Research Network
ISRN Signal Processing
Volume 2012, Article ID 614653, 8 pages
doi:10.5402/2012/614653

Research Article

Suboptimal Coherent Radar Detection in a *KK*-Distributed Clutter Environment

G. V. Weinberg

Electronic Warfare and Radar Division, Defence Science and Technology Organisation, Edinburgh, SA 5111, Australia

Correspondence should be addressed to G. V. Weinberg, graham.weinberg@dsto.defence.gov.au

Received 25 June 2012; Accepted 26 August 2012

Academic Editors: E. Ciaccio, F. Perez-Cruz, G. A. Tsihrintzis, and M. Wicks

The *KK*-Distribution is an important clutter model for high-resolution radar sea clutter returns obtained at X-band. The Neyman-Pearson optimal *KK* multilook detector has been derived recently, as well as the generalised likelihood ratio test suboptimal detector. Both these detectors are dependent on the modified Bessel-function of the second kind. This paper suggests a suitable suboptimal approach, using a well-known Bessel identity, eliminating the Bessel function dependence. This produces a computationally simpler detection scheme, whose performance is analysed using clutter parameters based upon real X-band radar returns.

1. Introduction

Coherent multilook radar detection is an area of much activity in radar signal processing research [1–6]. Much of the work undertaken in the literature is based upon a Neyman-Pearson likelihood detector, which requires the specification of an appropriate clutter model. Over the last three decades much focus has been on the K-Distribution, which superseded the earlier Gaussian, Lognormal, Rayleigh and Weibull models [5–8]. The K-Distribution was introduced to model observed features of real-sea-clutter returns. In particular, the K-Distribution models fast fluctuations of sea clutter using a conditional Rayleigh distribution, while the underlying modulation is modelled through a gamma distribution. The fast fluctuations are called the speckle, while the modulation is known as the texture [7, 8]. The K-Distribution, as an amplitude model, has density given by

$$f_K(t) = \frac{2c}{\Gamma(\nu)}\left(\frac{ct}{2}\right)^{\nu} K_{\nu-1}(ct), \tag{1}$$

where the parameter ν is referred to as the K-Distribution's shape parameter, while c is called the scale parameter. The shape parameter ν governs the tail of the K-Distribution's density, and it has been found that small values of ν ($\nu < 0.1$) represent more spiky clutter while larger values of ν ($\nu > 20$) produce backscattering that is closer to Rayleigh in distribution [9].

In order to improve the fit of the K-Distribution to real data, [10] proposed a mixture distribution version of the K-Distribution, known as the KK-Distribution. In this mixture model, two K-Distributions share the same shape parameter ν, but have different scale parameters c_1 and c_2. Its density, again in the amplitude domain, is given by the mixture

$$f_{KK}(t) = (1-k) f_{K_1}(t; c_1, \nu) + k f_{K_2}(t; c_2, \nu), \tag{2}$$

where each f_{K_j} is a K-Distribution with parameters as specified. The first K-Distribution density in (2) represents the Bragg and whitecap scatterers in the model. The second K-Distribution in (2) represents the spike component of the clutter. Parameter $k \in [0, 1]$ is called the mixing coefficient. Comparison of this model to high-resolution radar sea clutter has been recorded in [10], where it is shown that the KK-Distribution provides a better fit to the upper tail region of the empirical distribution than the K-Distribution. The KK-Distribution's validity is also supported by the analysis of trials data in [11], who also extend the model to include multiple looks and thermal noise.

The last few years has seen the emergence of the Pareto model for high-resolution radar maritime clutter returns obtained at X-band [1, 2, 12, 13]. In addition to this, clutter

models based upon an alpha-stable distribution have been proposed [14–16], which have a Pareto-like tail. However, the KK-Distribution still has an important role in radar, due to the fact that it provides a tighter fit in the upper tail region of the empirical distribution functions, as pointed out in [12, 13].

Recently, coherent multilook detection for targets embedded within a compound Gaussian model, whose marginal amplitude distributions are KK-Distributed, has been examined in [4]. In the latter, both the optimal Neyman-Pearson detector, and the generalised likelihood ratio test suboptimal decision rules, have been derived. These detectors have complex dependence on the modified Bessel function of the second kind. This paper uses a Bessel function identity to produce computationally simpler suboptimal detection schemes. The motivation for this is twofold. Firstly, an active radar must process a huge number of returns sequentially. Hence, it is important to reduce the computation time for each processed return, even if it is by a small amount. Secondly, for the implementation of a radar detection scheme in practice, it will be necessary to set the detection threshold for a given false-alarm probability. Thus, it is important to have an analytical relationship that is as simple as possible, to facilitate the determination of such thresholds.

The new detector's performance is examined relative to a clutter model whose parameters are estimated from real X-band high-resolution radar clutter returns. Thus, it will be assumed that the clutter parameters are completely known to the radar system.

The paper is arranged as follows. Section 2 outlines the coherent multilook detection problem, including the optimal Neyman-Pearson detector and generalised likelihood ratio test detector. Section 3 derives suboptimal detectors using Bessel function approximation. The performance of these suboptimal detectors is then analysed in Section 4.

2. Coherent Multilook Detection

It is necessary to first specify the clutter model used in the construction of the Neyman-Pearson optimal and suboptimal detectors. The following is based very closely on the problem formulation in [4], and is included for completeness. The clutter is modelled as a spherically invariant random process (SIRP) [17], which requires the specification of an appropriate characteristic function. Modelling clutter by such a process has been justified experimentally with real-radar clutter returns [18]. The appropriate SIRP, for the KK-clutter model, has N-dimensional complex clutter vector $\mathbf{c_v} = S\mathcal{G}$, where the nonnegative univariate random variable S has density given by

$$f_S(s) = (1-k) f_{S_1}(s) + k f_{S_2}(s), \tag{3}$$

where

$$f_{S_j}(s) = \frac{{c_j}^{2\nu}}{2^{2\nu-1}\Gamma(\nu)} s^{2\nu-1} e^{-{c_j}^2 s^2/4}, \tag{4}$$

for each $j \in \{1,2\}$ [4]. The N-dimensional process $\mathcal{G}$ is complex Gaussian with zero mean vector and covariance matrix Σ, which is assumed to be positive definite. This enables a whitening approach to be used to simplify the densities under each hypothesis in the Neyman-Pearson Lemma [4]. Central to the SIRP approach is the characteristic function, which is an integral component of densities used in the Neyman-Pearson Lemma. The function

$$h_N(u) = \frac{u^{(\nu-N)/2}\zeta(\sqrt{u}; c_1, c_2, \nu, k)}{\Gamma(\nu) 2^{1.5\nu+0.5N-1}} \tag{5}$$

with ζ defined by

$$\begin{aligned}\zeta(u; c_1, c_2, \nu, N, k) = {} & (1-k) c_1^{N+\nu} K_{N-\nu}(c_1 u) \\ & + k c_2^{N+\nu} K_{N-\nu}(c_2 u)\end{aligned} \tag{6}$$

has been shown to be the characteristic function of an SIRP that generates KK-Distributed marginal distributions, with shape parameter ν, scale parameters c_1 and c_2, and mixing coefficient k.

The coherent multilook detection problem is specified through the statistical test

$$H_0 : \mathbf{z} = \mathbf{c_v} \quad \text{against } H_1 : \mathbf{z} = R\mathbf{p} + \mathbf{c_v}, \tag{7}$$

where all complex vectors are $N \times 1$. The vector $\mathbf{z}$ is the radar return. H_0 is the null hypothesis (return is pure clutter), while H_1 is the alternative hypothesis (return consists of a mixture of signal and clutter). The vector $\mathbf{p}$ is the Doppler steering vector, which is assumed to be completely known, with components given by $\mathbf{p}(j) = e^{j2\pi i f_D}$, for $j \in \{1, 2, \ldots, N\}$, where $f_D \in [-0.5, 0.5]$ is the target normalised Doppler frequency. The complex random variable R is the target model and $|R|$ is the target amplitude. Since we are assuming that Σ is positive definite, it is convenient to apply a whitening process to the test (7). The validity of this is discussed in [4]. This means there exists a Cholesky factor matrix A such that $\Sigma^{-1} = A^H A$. Consequently, we can redefine $\mathbf{r} = A\mathbf{z}$, $\mathbf{n} = A\mathbf{c_v}$, and $\mathbf{u} = A\mathbf{p}$. The result is that the test (7) can be recast in the form

$$H_0 : \mathbf{r} = \mathbf{n} \quad \text{against } H_1 : \mathbf{r} = R\mathbf{u} + \mathbf{n}. \tag{8}$$

The Neyman-Pearson optimal detector is the ratio of the densities under H_1 and H_0 in (8), respectively [19]. For the case where the target variable R is fixed, it is shown in [4] that the likelihood ratio is given by

$$\begin{aligned} L(\mathbf{r}) &= \frac{h_N\left(\|\mathbf{r} - R\mathbf{u}\|^2\right)}{h_N\left(\|\mathbf{r}\|^2\right)} \\ &= \left(\frac{\|\mathbf{r} - R\mathbf{u}\|}{\|\mathbf{r}\|}\right)^{\nu-N} \frac{\zeta(\|\mathbf{r} - R\mathbf{u}\|; c_1, c_2, \nu, N, k)}{\zeta(\|\mathbf{r}\|; c_1, c_2, \nu, N, k)} \end{aligned} \tag{9}$$

with the optimal decision rule as follows

$$L(\mathbf{r}) \underset{H_0}{\overset{H_1}{\gtrless}} \tau, \tag{10}$$

where τ is the detection threshold. In (10), the notation $X \underset{H_0}{\overset{H_1}{\gtrless}} Y$ means that we reject the null hypothesis H_0 if and

only if $X > Y$. Given a radar return $\mathbf{r}$, the likelihood $L(\mathbf{r})$ is compared to the threshold τ in order to make a decision on whether a target signature is present in the return.

In a real application, the target is unknown and hence R must be estimated. If we assume R is unknown but constant from scan to scan, the generalised likelihood ratio test (GLRT) is used to first estimate this parameter, and then apply the estimate to the test (10). The methodology of GLRT is described in detail in [4]. As explained in the latter, the GLRT uses the approximation

$$\|\mathbf{r} - R\mathbf{u}\|^2 \approx \|\mathbf{r}\|^2 - \frac{\left|\mathbf{u}^H\mathbf{r}\right|^2}{\|\mathbf{u}\|^2} \tag{11}$$

in (9), to eliminate dependence on R, permitting the determination of (10) without target knowledge. In cases where the clutter parameters are also unknown, maxiumum likelihood estimates of these are also used in (9).

There is a large number of examples in the literature where approximations are applied to simplify (9) and (10); see [20] and references contained therein. The approach explored here is based upon a simple Bessel-function identity.

3. A Suboptimal Detector

The motivation for the development of a suboptimal version of (9) is that the Bessel function adds computational complexity to implemented detection schemes. As stressed earlier, a radar system will be processing a significantly large number of returns sequentially. Hence any reduction in computational cost will improve performance. A large number of such improvements, regardless of how small, will accumulate into an overall system performance saving.

A further motivation for this approach is to facilitate the construction of simple false-alarm probability/threshold relationships. It will also result in system savings if there is a simpler relationship to work with, between these two parameters. It was hence of interest to see whether any of the well-known Bessel identities could produce a suboptimal decision rule without incurring a significant detection loss. Bessel-function approximations have been addressed in a number of publications [21, 22]. A fixed-order approximation to the Bessel function was selected, in an attempt to keep the approximation as simple as possible. The following identity is the key to developing our suboptimal detector.

Lemma 1. *The modified Bessel function of the second kind, with order $\nu = 0.5$, is given by*

$$K_{0.5}(z) = \sqrt{\frac{\pi}{2}} e^{-z} z^{-1/2}, \tag{12}$$

where $z > 0$.

This can be found in [23] (equation 4.12.5, page 223).

In addition, the Lemma is exploited in [21] for similar purposes.

In view of (9), in cases where $N - \nu = 0.5$, this simplifies the optimal and GLRT detectors considerably. In terms of implementing a radar detection scheme, we can select an appropriate number of looks N so that the difference $N - \nu$ is as close as possible to 0.5.

If we assume $N - \nu = 0.5$, and define an auxiliary function

$$\eta(u; c_1, c_2, \nu, k) = (1-k)c_1^{2\nu} e^{-c_1 u} + k c_2^{2\nu} e^{-c_2 u} \tag{13}$$

then the function (6) reduces to

$$\zeta(u; c_1, c_2, \nu, N, k) = \sqrt{\frac{\pi}{2}} u^{-1/2} \eta(u; c_1, c_2, \nu, k) \tag{14}$$

with an application of (12). Using this result, the optimal detector specified by (9) and (10) simplifies to

$$L(\mathbf{r}) = \frac{\|\mathbf{r}\|}{\|\mathbf{r} - R\mathbf{u}\|} \frac{\eta(\|\mathbf{r} - R\mathbf{u}\|; c_1, c_2, \nu, k)}{\eta(\|\mathbf{r}\|; c_1, c_2, \nu, k)} \underset{H_0}{\overset{H_1}{\gtrless}} \tau. \tag{15}$$

In cases where $N - \nu \neq 0.5$, the decision rule (15) can be applied as a suboptimal detector. The expression (11) can also be applied to (15) to produce a corresponding GLRT version of (15). When it can be applied, the detector (15) is a computationally cheaper solution than that provided by (10).

To illustrate this, the two functions (6) and (14) are compared, in terms of their computation times. Consider the case where the clutter has parameters $\nu = 8.315$, $c_1 = 25$, and $c_2 = 26.5$ with $k = 0.01$. Figure 1 shows computation times (in a logarithmic scale) for the function (6) and its approximation by (14), for two number of looks ($N = 5$ and 8). This shows (14) can introduce a small saving computationally. Although this is a small reduction in time, millions of such computations will result in an overall improvement in performance. Varying N does not significantly alter the computation times from the two examples illustrated in Figure 1.

As a second example, the case where $\nu = 4.684$, $c_1 = 10$, $c_2 = 57.70$, with $k = 0.01$ is examined. Figure 2 shows the computational times for $N = 3$ and $N = 5$ looks. Again we observe that (14) has periods where it can introduce a computation saving. A somewhat unsurprising result is that when $N - \nu = 0.5$, similar plots show that (14) has a smaller computation time on average than (6).

Hence, there is computational validity in using (14) to approximate (6). It is now necessary to investigate the detection loss in using this approximation.

4. Performance of the Suboptimal Detector

4.1. Preliminaries. The critical question now is whether detectors based upon (15), using (12) as an approximation, can provide a small enough detection loss to merit the computational gain in using a simpler decision rule. This issue is examined here using detection performance curves, which plot the probability of detection as a function of signal to-clutter ratio (SCR).

A Gaussian or Swerling 1 target model is used in the numerical analysis to follow, as in [4]. In this case, the SCR is given by

$$\text{SCR} = \frac{\sigma^2 \|\mathbf{u}\|^2}{2N\nu\left[(1-k)/c_1^2 + k/c_2^2\right]}, \tag{16}$$

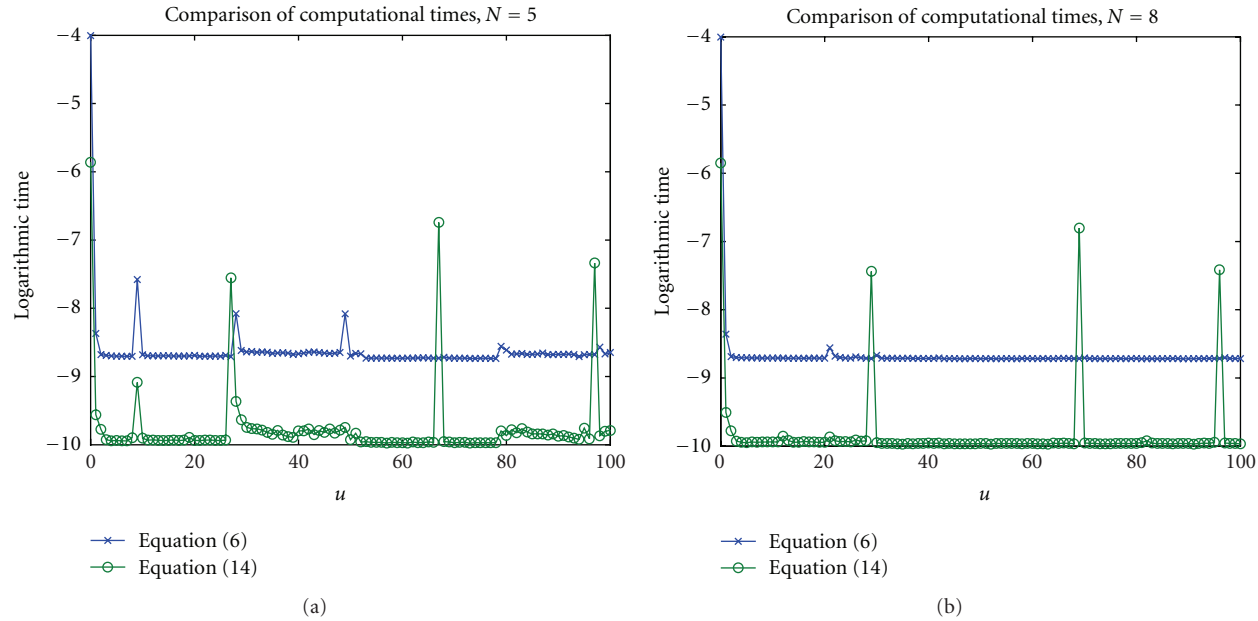

Figure 1: Examples of computation time for the expression (6) and its approximation (14).

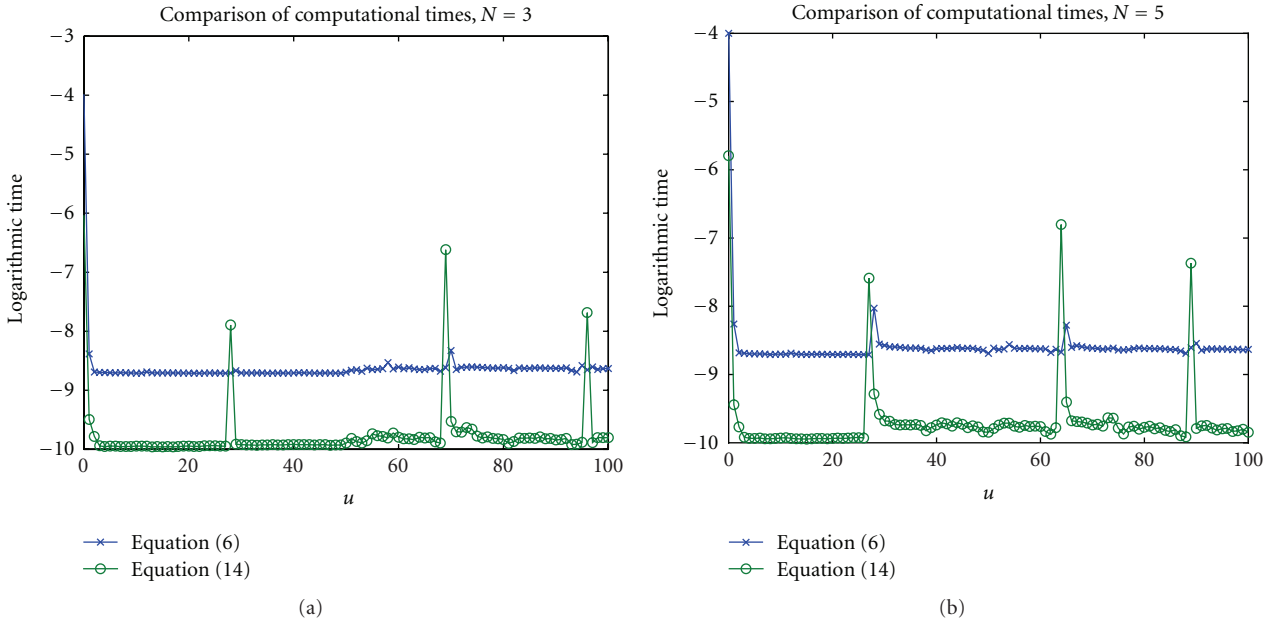

Figure 2: Further examples of the computational time of expression (6) compared to its approximation (14).

where in the context of the target model formulated in Section 2, $\mathbb{E}|R|^2 = 2\sigma^2$ for some $\sigma > 0$.

For each example considered, the clutter parameter set $\{c_1, c_2, \nu\}$ is based upon DSTO's high-resolution radar clutter sets generated by the Ingara radar operating in a trial in 2004. The Ingara radar is an X-Band fully polarised radar, which operated in a circular spotlight mode during the clutter gathering exercise. The trial was conducted in the Southern Ocean, roughly 100 km south of Port Lincoln in South Australia. Full details of this trial, the Ingara radar, and data analysis of the clutter returns obtained can be found in [9, 10, 24, 25]. Some key points, taken from [4], are reiterated. The radar viewed the same patch of sea surface at different azimuth angles. It used a centre frequency of 10.1 GHz, with 20 μs pulse width. Additionally, the radar operated at an altitude of 2314 m for a nominal incidence angle of 50°, and at 1353 m for 70° incidence angle. The trial collected data at incidence angles varying from 40° to 80°, on 8 different days over an 18 day period. As in [10], we focus on data from two particular flight-test runs. These correspond

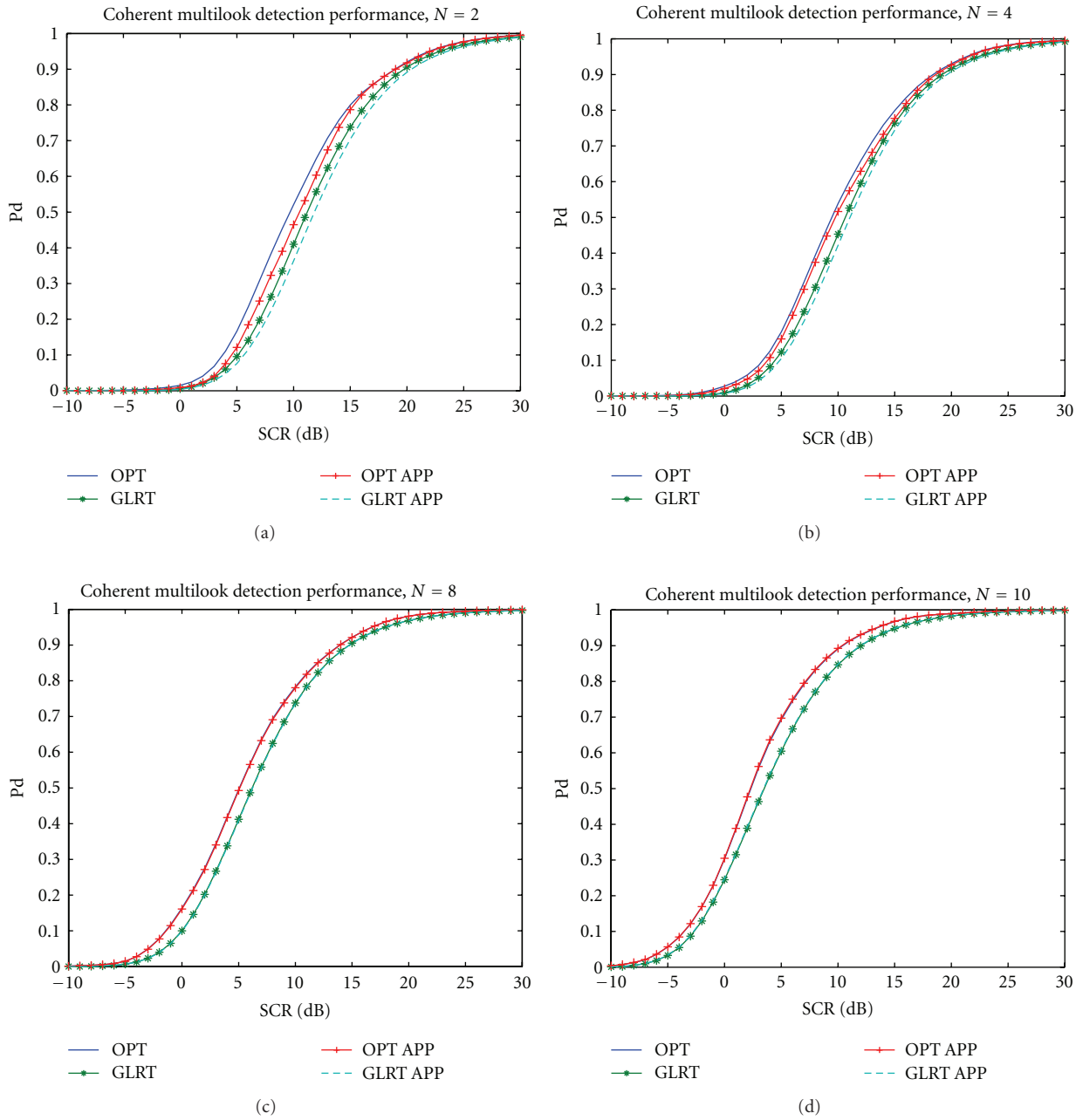

Figure 3: Detector performance curves based upon run 34690, azimuth angle 45°, vertical polarisation. Shown is the performance of the optimal detector (denoted OPT), the GLRT (with same label), the suboptimal approximation of the optimal detector (OPT-APP), and the suboptimal approximation of the GLRT (GLRT-APP).

to run 34683 and run 34690, which were collected on 16 August 2004 between 10 : 52 am and 11 : 27 am local time [10]. Dataset run 34683 was obtained at an incidence angle of 51.5°, while run 34690 was at 67.2°. Each of these datasets were also processed in blocks to cover azimuth angle spans of 5° over the full 360° range. Roughly 900 pulses were used, and 1024 range compressed samples for each pulse were produced, at a range resolution of 0.75 m. In [10] parameter estimates for the datasets run 34683 and run 34690 are given, enabling the fitting of the K- and KK-Distributions to this data. This will be employed in the numerical analysis to follow. Further details on the clutter model fitting can be found in [10]. As reported in the latter, the radar is facing upwind at approximately 227° azimuth, which is the point of strongest clutter. Downwind is at approximately 47°, which is the point where the clutter is weakest. Crosswind directions are encountered at 137° and 317° approximately.

The clutter covariance matrix is chosen to have a Toeplitz structure. This means we assume the matrix Σ has (i, j)th element given by $\Sigma(i, j) = \kappa^{|i-j|}$, for i and j taking values from 1 to the maximum number of looks. The Toeplitz factor

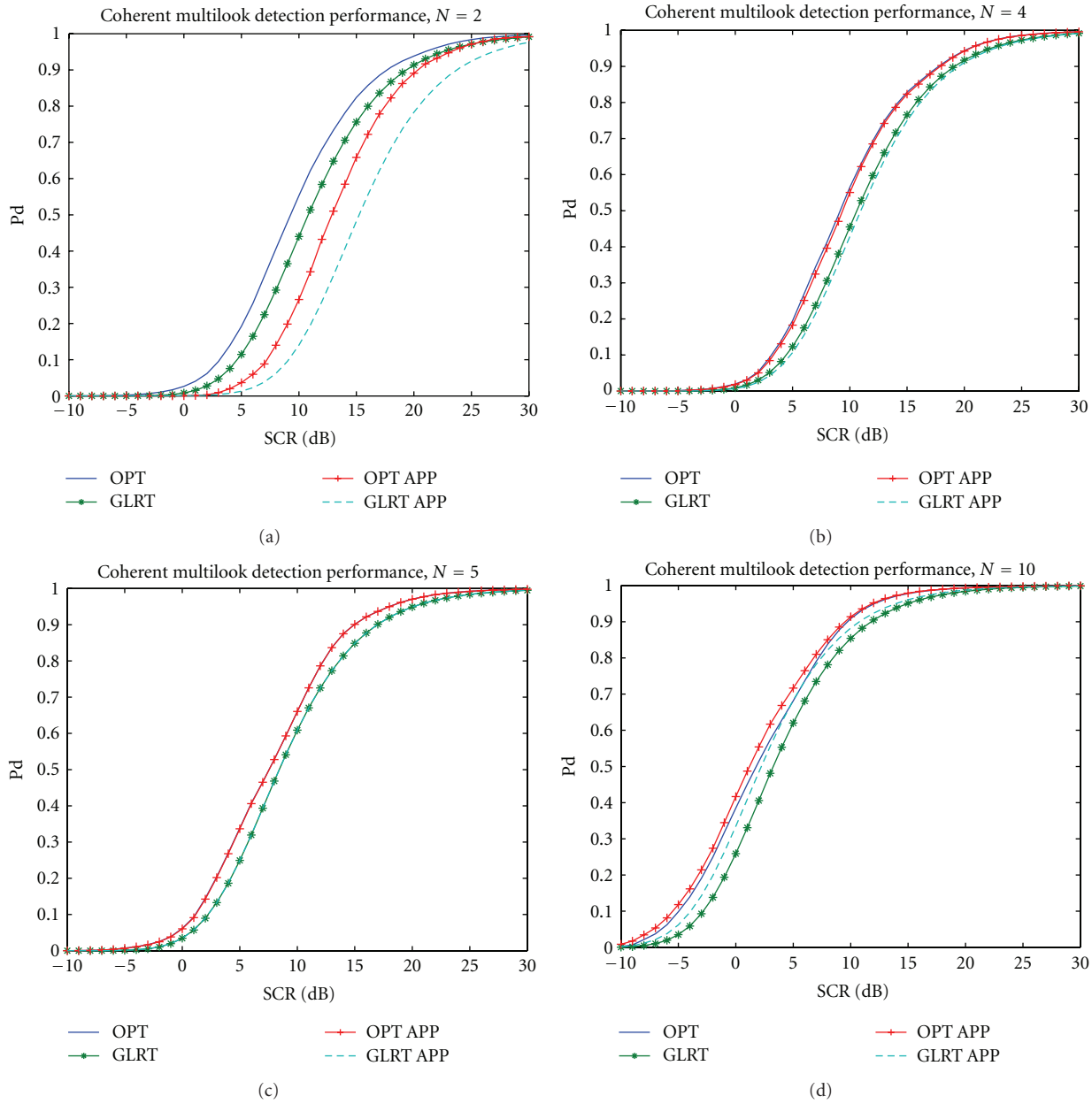

Figure 4: Performance of the new suboptimal detectors relative to the optimal and GLRT detectors. This example has been based upon clutter parameters estimated from dataset run 34683, azimuth angle 190°, with horizontal polarisation.

κ is between 0 and 1. Throughout it has been set to 0.8, to reflect strong clutter returns. In addition, the false alarm probability has been set to 10^{-6}. The normalised Doppler frequency is $f_D = 0.5$ in all examples. The KK-mixing coefficient has been set to $k = 0.01$, as reflected by the clutter parameter fits in [10].

All detection performance curves have been produced using Monte Carlo simulation, with each data point estimated using at least 10^6 runs.

4.2. Example 1. The first example considered has been based upon the DSTO dataset run 34690, which was obtained at an azimuth angle of 45°, with vertical polarisation. This is only 2° from the downwind direction. The fitted KK-Distribution parameters are $\nu = 8.315$, $c_1 = 25$, and $c_2 = 26.5$. Figure 3 shows four detection performance curves for this case, where the number of looks N is varied. The top left subplot is for $N = 2$, the top right subplot corresponds to $N = 4$, the bottom left subplot has $N = 8$, while the bottom right subplot is for $N = 10$. Shown in all subplots is the performance of the optimal detector (10), the GLRT ((10) using (11)), as well as suboptimal approximations based upon (15). The Figure shows the latter applied to the optimal detector directly (denoted OPT APP), as well as to the GLRT (denoted GLRT APP). What is evident from Figure 3 is that

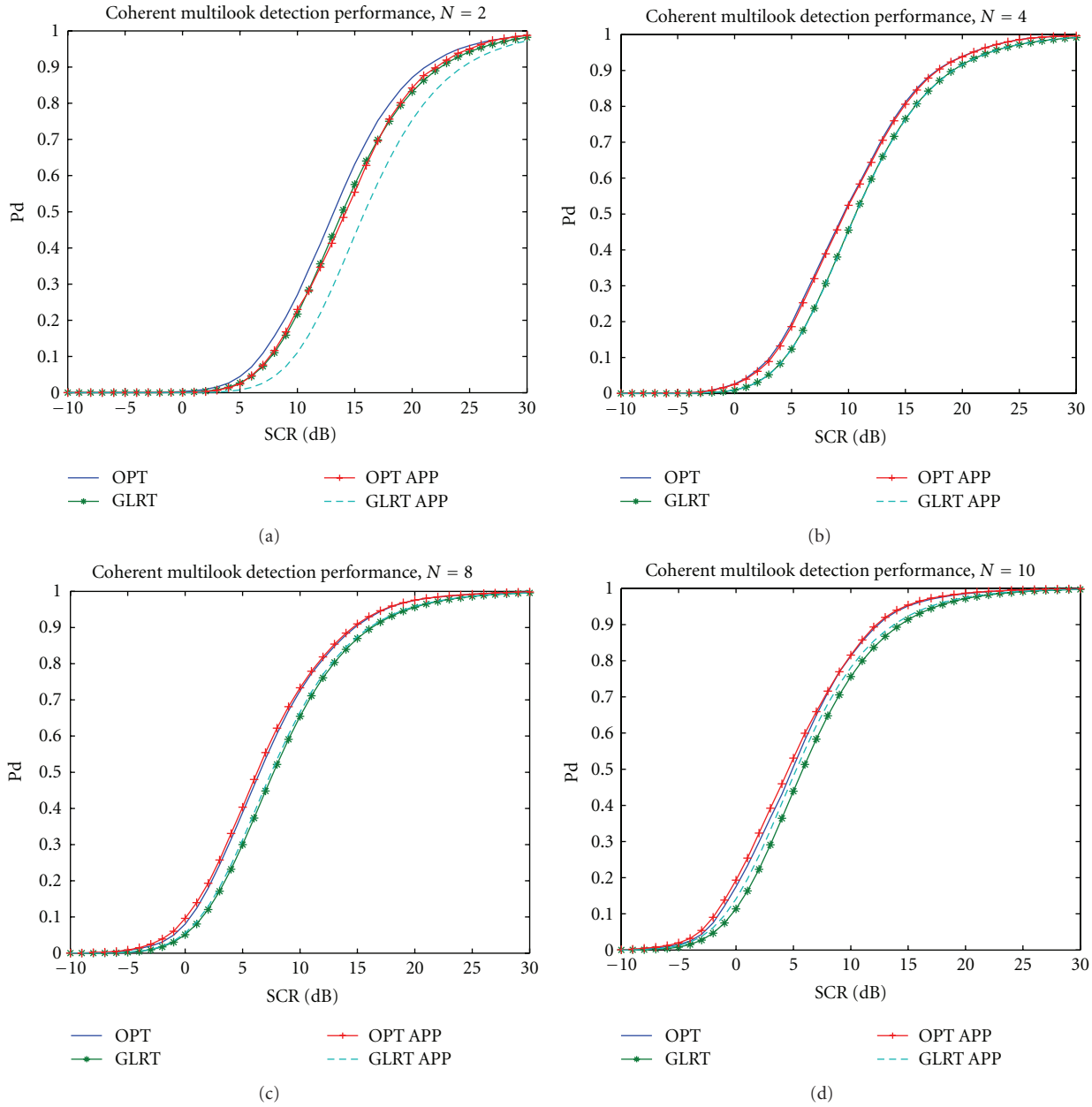

FIGURE 5: Detector performance in an almost upwind scenario, based upon dataset run 34683, azimuth angle 225°, with horizontal polarisation. The detection loss by using the new suboptimal detectors is not as significant as the example investigated in Figure 4.

the new suboptimal detector performs very well, with an almost negligible detection loss in all cases illustrated.

4.3. Example 2. The second example is for the case where the *KK* shape parameter is $\nu = 4.684$, and the scale parameters are $c_1 = 10$ and $c_2 = 57.70$, respectively. These are based upon the dataset run 34683, at an azimuth angle of 190°, with horizontal polarisation. In Figure 4, the number of looks is varied from $N = 2$ (top left subplot), $N = 4$ (top right subplot), $N = 5$ (bottom left subplot), and $N = 10$ (bottom right subplot). For the case where $N = 2$, we observe there is a significant detection loss between the optimal detector/GLRT and their suboptimal versions. For a fast scanning radar, where only a few pulses may be received, this means we would incur a significant detection loss in using (15). As the number of looks is increased, the performance of detectors based upon (15) improves as shown.

4.4. Example 3. The final example, illustrated in Figure 5, is also for horizontal polarisation. Clutter parameters have been estimated from dataset run 34683 as previously, but with an azimuth angle of 225°. This is only 2° from the upwind direction. Clutter parameter estimates, based upon [10], are $\nu = 4.158$ (shape parameter) and $c_1 = 5.5$,

$c_2 = 17.985$ (scale parameters). The number of looks is cycled through $N = 2$, 4, 8, and 10 as illustrated in Figure 5. The performance shown in Figure 5 is similar to that in Figure 4, except that the detection loss at small number of looks is not as significant as that in Figure 4.

5. Conclusions and Further Research

Using a Bessel-function approximation, two new suboptimal detectors were produced, and their performance was gauged against the Neyman-Pearson optimal detector, as well as the generalised likelihood ratio test detector. It was shown that the function (14) introduced a minor computational saving over (6), which would result in overall system performance improvement when a huge number of radar returns are sequentially processed. The validity of this approximation was explored using detection performance curves, with clutter parameters estimated from DSTO's Ingara data, with a Gaussian target model. It was shown small detection losses are possible in a number of cases. In particular, the number of looks can be chosen so that the difference between it and the KK-shape parameter is as close as possible to 0.5. For a large number of looks, as in the case where the radar's scan rate is slow to medium, the new suboptimal approximations can be used without a large detection loss.

Further work will be spent trying to determine the probability of false alarm and threshold relationship, through an analytic expression, which is vital for the real-time implementation of these detection schemes.

References

[1] K. J. Sangston, F. Gini, and M. S. Greco, "Coherent radar target detection in heavy-tailed compound Gaussian clutter," *IEEE Transactions on Aerospace and Electronic Systems*, vol. 48, no. 1, pp. 64–77, 2012.

[2] X. Shang and H. Song, "Radar detection based on compound-Gaussian model with inverse gamma texture," *IET Radar, Sonar and Navigation*, vol. 5, no. 3, pp. 315–321, 2011.

[3] G. V. Weinberg, "Coherent multilook radar detection for targets in pareto distributed clutter," *Electronics Letters*, vol. 47, no. 14, pp. 822–824, 2011.

[4] G. V. Weinberg, "Coherent multilook radar detection for targets in KK-distributed clutter," in *Digital Communication*, C. Palanisamy, Ed., Intech, Zagreb, Croatia, 2012.

[5] Y. Dong, "Optimal coherent radar detection in a K-distributed clutter environment," *IET Radar, Sonar & Navigation*, vol. 6, no. 5, pp. 283–292, 2012.

[6] F. Gini, M. V. Greco, A. Farina, and P. Lombardo, "Optimum and mismatched detection against K-distributed plus gaussian clutter," *IEEE Transactions on Aerospace and Electronic Systems*, vol. 34, no. 3, pp. 860–876, 1998.

[7] K. D. Ward, "Compound Representation of High Resolution Sea Clutter," *Electronics Letters*, vol. 17, no. 16, pp. 561–563, 1981.

[8] K. D. Ward, S. Watts, and R. J. A. Tough, *Sea Clutter: Scattering, the K-Distribution and Radar Performance*, IET Radar, Sonar & Navigation, Series 20, IET, London, UK, 2006.

[9] D. J. Crisp, L. Rosenberg, N. J. Stacy, and Y. Dong, "Modelling X-band sea clutter with the K-distribution: shape parameter variation," in *Proceedings of the IEEE International Conference on Surveillance for a Safer World (RADAR '09)*, Bordeaux, France, December 2009.

[10] Y. Dong, "Distribution of X-band high resolution and high grazing angle sea clutter," DSTO Report RR-0316, 2006.

[11] L. Rosenberg, D. J. Crisp, and N. J. Stacy, "Analysis of the KK-distribution with medium grazing angle sea-clutter," *IET Radar, Sonar and Navigation*, vol. 4, no. 2, pp. 209–222, 2010.

[12] M. Farshchian and F. L. Posner, "The pareto distribution for low grazing angle and high resolution X-band sea clutter," in *Proceedings of the IEEE International Radar Conference (RADAR '10)*, pp. 789–793, May 2010.

[13] G. V. Weinberg, "Assessing Pareto fit to high-resolution high-grazing-angle sea clutter," *Electronics Letters*, vol. 47, no. 8, pp. 516–517, 2011.

[14] G. A. Tsihrintzis, M. Shao, and C. L. Nikias, "Recent results in applications and processing of α-stable-distributed time series," *Journal of the Franklin Institute*, vol. 333, no. 4, pp. 467–497, 1996.

[15] G. A. Tsihrintzis and C. L. Nikias, "Evaluation of fractional, lower-order statistics-based detection algorithms on real radar sea-clutter data," *IEE Proceedings Radar, Sonar and Navigation*, vol. 144, no. 1, pp. 29–38, 1997.

[16] G. A. Tsihrintzis and C. L. Nikias, "Data-adaptive algorithms for signal detection in sub-gaussian impulsive interference," *IEEE Transactions on Signal Processing*, vol. 45, no. 7, pp. 1873–1878, 1997.

[17] M. Rangaswamy, D. Weiner, and A. Oeztuerk, "Non-Gaussian random vector identification using spherically invariant random processes," *IEEE Transactions on Aerospace and Electronic Systems*, vol. 29, no. 1, pp. 111–124, 1993.

[18] E. Conte and M. Longo, "Characterisation of radar clutter as a spherically invariant random process," *IEE proceedings F*, vol. 134, no. 2, pp. 191–197, 1987.

[19] G. P. Beaumont, *Intermediate Mathematical Statistics*, Chapman and Hall, London, UK, 1980.

[20] E. Conte, M. Lops, and G. Ricci, "Asymptotically optimum radar detection in compound-Gaussian clutter," *IEEE Transactions on Aerospace and Electronic Systems*, vol. 31, no. 2, pp. 617–625, 1995.

[21] F. Aluffi Pentini, A. Farina, and F. Zirilli, "Radar detection of targets located in a coherent K distributed clutter background," *IEE Proceedings F*, vol. 139, no. 3, pp. 239–245, 1992.

[22] E. J. Weniger and J. Cížek, "Rational approximations for the modified Bessel function of the second kind," *Computer Physics Communications*, vol. 59, no. 3, pp. 471–493, 1990.

[23] G. E. Andrews, R. Askey, and R. Roy, *Special Functions*, Cambridge University Press, Cambridge, UK, 2000.

[24] N. J. S. Stacy and M. P. Burgess, "Ingara: the Australian airborne imaging radar system," in *Proceedings of the 1994 International Geoscience and Remote Sensing Symposium*, pp. 2240–2242, August 1994.

[25] N. J. S. Stacy, D. Crisp, A. Goh, D. Badger, and M. Preiss, "Polarimetric analysis of fine resolution X-band SAR sea clutter data," in *Proceedings of the IEEE International Geoscience and Remote Sensing Symposium (IGARSS '05)*, pp. 2787–2790, July 2005.